PARAMETERIZATIONS OF SOLAR SINGLE-SCATTERING
RADIATIVE PROPERTIES FOR TROPICAL ICE CLOUDS

Greg M. McFarquhar[1], Ping Yang[2], Andreas Macke[3],
Anthony Baran[4], Sam Iacobellis[5], and Richard Somerville[5]

[1]University of Illinois at Urbana-Champaign, Urbana, IL,
[2]Texas A&M University, College Station, TX,
[3]University of Kiel, Cologne, Germany,
[4] Met Office, Bracknell, UK,
[5]Scripps Institution of Oceanography, La Jolla, CA

1. INTRODUCTION

Ice clouds, especially cirrus, have been shown in general circulation model (GCM) and satellite studies to have a major effect on the Earth's radiation balance and climate as a result of the significant contribution they make to the diabatic heating of the upper troposphere. An accurate description is needed not only of the cloud microphysics, but also of cloud-radiative interactions. The weakest physical link for the representation of microphysics and radiation in cloud and larger scale models are their connected descriptions. Because of complex non-linear interactions between radiation and microphysics, it has been necessary to parameterize or simplify the results of detailed radiative transfer models for incorporation into cloud and larger scale models.

Many parameterizations of the short-wave optical properties of ice clouds in terms of ice water content (IWC), effective radius (r_e), and temperature have been developed (e.g., Ebert and Curry 1992; Fu 1996) assuming various ice crystal shapes. Discrepancies between schemes may be significant because radiative flux calculations substantially depend on parameterizations of shortwave solar properties (Vogelman and Ackerman 1995). Differences exist between schemes due to variations in the treatment of radiative transfer codes and, more importantly, due to assumptions about ice crystal shape.

In this study, a new parameterization of solar single-scattering radiative properties is developed for tropical anvils by combining in-situ observations of ice crystal size and shape with a library of single-scattering properties derived using an improved geometric ray-tracing code (Yang et al. 2000, hereafter Y00). Improvements over previous studies are obtained by explicitly accounting for the numbers, shapes, and sizes of small crystals, by using observed mixtures of habits (rather than assuming single habits), and by accounting for potential variances in fit coefficients. Simulations with the Scripps single-column model (SCM, Iacobellis and Somerville 2000) are used to determine how uncertainties in the fit coefficients scale up to uncertainties in cloud radiative forcing (CRF).

Corresponding author address: Greg M. McFarquhar, University of Illinois, Dept. of Atmospheric Sciences, 105 S. Gregory Street, Urbana, IL, 61801-3070, mcfarq@atmos.uiuc.edu

2. PARAMETERIZATION TECHNIQUE

During the Central Equatorial Pacific Experiment (CEPEX), 35 hours of microphysical measurements were collected in blowoff anvils associated with deep convection using a Learjet. A two-dimensional cloud (2DC) probe was used to measure large ice crystals, with maximum dimensions (D_{max}) larger than 120 μm. Habit-dependent size distributions were calculated using a neural-network classification scheme (McFarquhar et al. 1999, hereafter M99), based on the maximum dimension and area ratio of each image; each crystal was identified as a column, bullet rosette, or aggregate. Because the 2DC does not accurately measure small crystals, a size distribution of small crystals, calculated using McFarquhar and Heymsfield's (1997, hence MH97) parameterization based upon measurements collected by the Video Ice Particle Sampler (VIPS), was added to each observed distribution. The mass contained in the small crystal sizes was chosen by randomly choosing coefficients from MH97 using a bootstrap technique that reflects the wide range in small crystal numbers observed (McFarquhar et al. 2002). Because over 90% of 11,000 small crystal images were manually identified as quasi-spherical, Chebyshev particles were chosen to represent their shapes. The coefficients of the Chebyshev polynomials were chosen so that the projected area of the idealized crystals was equal to the projected area of the imaged crystals.

To calculate the mean single-scattering properties of these distributions, the size and shape information from the microphysics distributions is combined with radiative properties calculated for specific shapes and sizes of ice crystals. Y00 describe GOM2, which is used to provide the radiative properties of specific shapes and sizes of ice crystals for the 56 different visible and near-infrared wavelengths listed in Table 1 of Y00. For size parameters on the order of 15-20, this method provides more accurate results than the conventional ray-by-ray Monte Carlo ray tracing technique that has traditionally been used to calculate scattering properties. The calculated radiative properties assume that the crystals are randomly oriented in space. The GOM2 library of radiative properties is available for the following shapes: rough and smooth aggregates, hexagonal columns and plates, bullet rosettes

and dendrites. The radiative properties for the Chebyshev particles are calculated by means of the ray-tracing method (Macke and Grossklaus 1998). These routines accurately calculate the single-scattering properties and scattering phase functions for the wavelengths and particle sizes under consideration. The small ice crystals are also randomly oriented in three-dimensional space.

To combine the scattering properties for different sizes and shapes of ice crystals, the scattering properties of individual ice crystals are weighted by scattering cross-section and number concentration following the techniques used by M99, Y00, and others. The scattering properties are computed for the 56 different wavelengths, and then combined into the 4 broadbands used by CCM3 (0.25-0.69, 0.69-1.19, 1.19-2.38, and 2.38-4.0 μm) and other climate models, weighted according to the fraction of solar irradiance at the top of atmosphere in each band.

3. RESULTS

The scattering phase functions for the merged size and shape distributions are smooth and featureless when compared to the functions for pristine crystals, such as columns and bullet rosettes. This matches the featureless nature of Baran et al.'s (2001) analytic phase function, which is based on laboratory measurements of scattering from distributions of ice crystals. However, there are differences, as the phase functions calculated here have a pronounced backscatter peak not seen in the analytic phase function, probably due to contributions from the pristine habits. Hence, there may be differences in the bulk single-scattering properties, which are used in climate models (e.g., asymmetry parameter g, single-scattering albedo ω_0, extinction coefficient β_{ext}), derived from these representations of phase function.
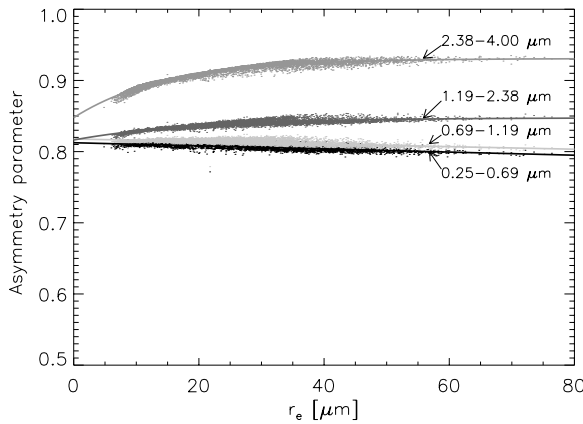

Figure 1: Asymmetry parameter as function of r_e for 4 wavelength bands used by Scripps SCM. Data points represent values obtained by combining composite size distributions, obtained from optical array probe data and small crystal parameterization, with improved geometric ray-tracing technique.

Figure 1 plots g as a function of r_e for the four different wavelength bands used by CCM3. Each point corresponds to the calculated g for an observed size and shape distribution during CEPEX, with small crystal contributions added. The scatter in g occurs due to

variation in mixtures of habits making up crystal distributions and due to the variation in small crystal contributions due to the random application of MH97. Additional plots showed that using temperature or IWC to stratify the data does not reduce the scatter.

To determine a functional representation characterizing the g-r_e relationship, fits are performed using a non-linear Levenberg-Marquardt technique. Different functions represent g for different wavelength bands, with

$$g = \begin{cases} a_i + b_i r_e, i = 1,2 \\ a_i + b_i \exp(-c_i r_e), i = 3,4 \end{cases} \quad (1)$$

where i=1,2 refers to the 0.25-0.69 and 0.69-1.19 μm bands and i=3,4 refers to the 1.19-2.38 and 2.38-4.0 μm bands. The coefficients a_i, b_i, and c_i are wavelength dependent. Note that c_i=0 for i=1 or 2. Separate functions are needed for the different bands because convergence was not obtained for exponential fits to the first two bands and an exponential is required to characterize the decrease in g for small r_e for higher bands. Similar fits and procedures were followed to quantify relationships between ω_0 and r_e, and between β_{ext} and r_e.

The coefficients a_i, b_i, and c_i are not represented by single values, but rather are represented by a two-dimensional ellipse or three-dimensional ellipsoid in the phase space of the fit parameters. The principal axis of the ellipse/ellipsoid is determined from the eigenvalues and eigenvectors of the inverse of the covariance matrix. The boundary of the ellipse/ellipsoid is determined by setting $\Delta\chi^2 = \chi^2 - \chi^2_{min}$. χ^2_{min} is the minimum chi-squared calculated for the most likely fit coefficients, and χ^2 represents chi-squared for fit coefficients that lie on the ellipse/ellipsoid boundaries, representing extreme values of acceptable fit coefficients. $\Delta\chi^2$ is chosen to encompass a 99% confidence interval ($\Delta\chi^2 = 9.21$ in 2 dimensions and $\Delta\chi^2 = 11.3$ in 3 dimensions).
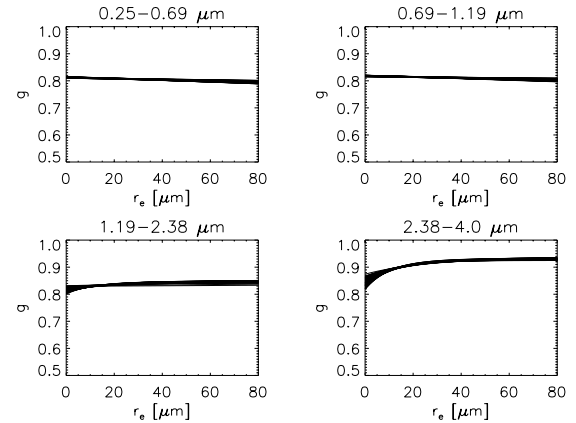

Figure 2: Asymmetry parameter as function of re obtained by parameterization. Different lines represent parameterizations obtained by randomly choosing different fit coefficients from the surface of possible solutions.

Figure 2 shows different realizations of g-r_e relations determined by randomly choosing coefficients from the ellipse/ellipsoid. Similar trends are noted for all curves regardless of coefficient choice. For most λ, there is a

scatter in g of up to approximately .02 depending on r_e. There is even greater uncertainty in g for small r_e for bands 3 and 4. These uncertainties may be high enough to impact radiative fluxes up to Vogelman and Ackerman's (1995) flux criterion of +/-5%, especially for large optical depths. By choosing larger or smaller $\Delta\chi^2$ in deriving the ellipse/ellipsoid, this spread could be either increased or reduced accordingly.

The surfaces calculated above give some information about variations in fit coefficients that may represent natural variations, or may represent behavior not well enough understood to parameterize. There are other uncertainties not included in the representations of these surfaces. Some of the more important sources may be errors due to the idealized models used to characterize crystal shapes, due to assumptions on the numbers and masses of small crystals, and due to uncertainties in the detection and measurement of all sized ice crystals. The methods used to calculate the radiative properties of the idealized crystals may also affect the results.
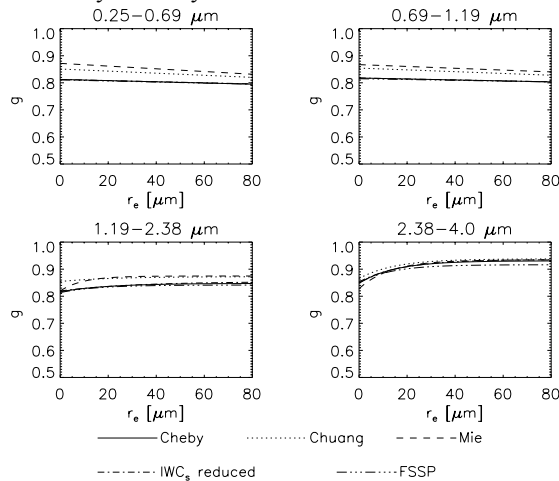

Figure 3: Comparison of g-re parameterizations obtained by representing deformed spheres by different shapes: eight order Chebyshev polynomials (solid lines), Chuang-Beard tenth order expansion of Chebyshev polynomials (dashed lines), and spheres with radiative properties determined by Mie theory (dotted lines). Dash-dot curve represents calculations limiting mass of small ice crystals when total IWC exceeds 0.1 g m-3, and FSSP represents parameterization obtained assuming that the FSSP can adequately measure small ice crystals (hence overestimating small crystal concentrations).

Figure 3 compares g-r_e relations predicted using three different shapes to describe the small crystals: eighth degree Chebyshev polynomials used for base simulations, tenth order expansion of Chebyshev polynomials used by Chuang and Beard (1990) to represent raindrop shapes scaled down to ice crystal sizes, and spheres with radiative properties determined by Mie theory. Differences between curves are greater than internal uncertainties associated with the parameterization, showing sensitivity to the assumed shapes of small crystals. For example, g can differ by up to .06 for different curves for the lowest two λ bands; differences are not as substantial for the higher λ bands, especially 2.38-4.0 μm. Preliminary calculations show that representing small crystals as Koch fractals

(figure not shown) can cause substantial differences in radiative properties of small crystals.

Figure 3 shows two other curves that describe changes in the parameterizations caused by minimizing or maximizing possible numbers of small crystals, according to uncertainties in the observations of small crystals. Some curves are not visible when they are directly underneath other curves. The curve that limits the mass of the small crystals does not substantially differ from the base parameterization because only 10% of the points in the sample had such large mass contents, because changes in r_e offset changes in g for such points, and because the numbers of the smallest crystals (D < 20 μm) did not change significantly. For the parameterizing maximizing possible numbers of small crystals, it is assumed that a forward scattering spectrometer probe (FSSP), whose performance in clouds with large ice crystals is uncertain, can adequately characterize the small crystals; however, it is seen that whether the VIPS or FSSP is used to measure the small crystals does not significantly impact parameterizations for g. This may be related to a saturation effect that occurs when the numbers of small crystals increases beyond some threshold.

Similar analysis and parameterizations were produced to describe ω_0 and Q_{ext}. Comparison with previous climate studies was made, and differences existed due to varying particle shape and the use of different radiative codes. Two significant results found were that: 1) although ω_0 does not depend significantly on choice of pristine habit for large crystals or on the choice of deformed sphere for small quasi-spherical particles, there are substantial differences in ω_0 between the deformed spheres and the large pristine ice crystals, the explanation of which is not fully understood at this time; 2) there are differences in the parameterizations developed here from those developed using other methods (Baran et al. 2000; Macke et al. 1996) designed to account for mixtures of ice crystal shapes and sizes. It cannot be currently resolved which model best represents tropical ice cloud radiative properties.

A bulk parameterization was also developed to describe the dependence of r_e on ice water content (IWC) using the same in-situ observations, with small crystal contributions again added by the stochastic application of MH97. There was a range in possible fit coefficients to reflect the fact that r_e can vary significantly about its mean value.

4. MODELING SIMULATIONS

The Scripps single column model (SCM) described by Iacobellis and Somerville (2000) is used to test the sensitivity of climate model simulations to the use of the new parameterization for r_e. In particular, it is determined how uncertainties in r_e scale up to uncertainties in modeled cloud and radiative properties. The simulations describe, and are based upon, conditions measured at the Atmospheric Radiation Measurement (ARM) program's Tropical Western Pacific (TWP) site, located in the area roughly between 10°N to 10°S from Indonesia to near Christmas Island in the warm pool region. A period

between 9 August 2000 and 8 September 2000 is simulated because data collected by the millimeter-wavelength cloud radar at Nauru Island (167°E, 2°S) indicated moderate cirrus activity then. Further, SCM simulations conducted over the entire second half of 2000 and all of 2001 indicated that high cloud cover and high cloud optical depth were near a maximum at this time. Forcing data were derived from the National Center for Environment Prediction's Global Spectral Model. Since these data are from a forcing model, and not observations, the forcing might be less accurate; however, preliminary indications are that the SCM is performing adequately.
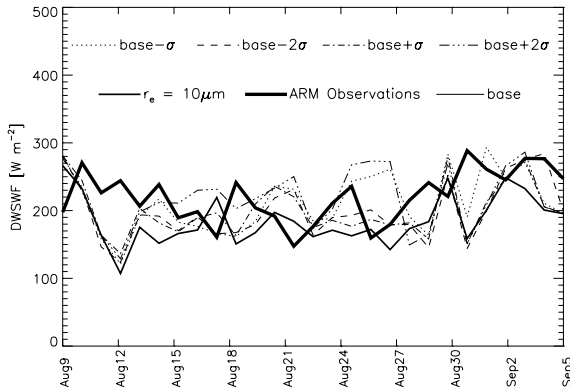

Figure 4: Temporal variation of downwelling shortwave flux (DWSWF) for 30-day time period of ARM TWP simulation. Different line types correspond to use of different r_e parameterizations as indicated in the legend. Medium thick lines represent simulation with r_e of 10 μm, and very thick lines represent observations acquired at the ARM TWP site.

Figure 4 compares the downwelling shortwave radiative flux at the surface as a function of time for simulations that used the base parameterization for r_e, and also for simulations that used parameterizations representing r_e values one and two standard deviations greater than and less than the mean r_e. Observations from the ARM TWP site are shown to put the simulations in perspective. It can be seen that there are substantial differences between the simulations at times, as caused by variations in r_e affecting the amount of reflected solar radiation and by differences in cloud heating rates. Further analysis (not shown) determined that the shortwave cloud radiative forcing could differ by as much as 17.7 W m^{-2} depending on the r_e parameterization coefficients used, showing that uncertainties in the coefficients may have a significant impact on modeled cloud and radiative properties.

5. SUMMARY

New parameterizations of the single-scattering solar radiative and microphysical properties have been deduced using a combination of in-situ observations and results of detailed radiative transfer codes. Their use may be appropriate in large-scale models to describe the properties of tropical anvils produced by deep convection. As with all parameterizations, caution must be taken if it is to be applied under conditions that differ from those under which the original data were collected. Ongoing studies are concentrating on determining whether similar parameterizations can be produced for Arctic and mid-latitude clouds.

7. REFERENCES

Baran, A.J., P.N. Francis, L. C.-Labonnote, M. Doutriaux-Boucher, 2001: A scattering phase function for ice cloud: Tests of applicability using aircraft and satellite multi-angle multi-wavelength radiance measurements of cirrus. *Quart. J. Roy. Meteor. Soc.*, **127**, 2395-2416.

Chuang, C.C., and K.V. Beard, 1990: A numerical model for the equilibrium shape of electrified raindrops. *J. Atmos. Sci.,* **47**, 1374-1389.

Ebert, E.E., and J.A. Curry, 1992: A parameterization of ice cloud optical properties for climate models. *J. Geophys. Res.*, **97**, 3831-3836

Fu, Q., 1996: An accurate parameterization of the solar radiative properties of cirrus clouds. *J.Climate*, **9**, 2058-2082.

Iacobellis, S.F., and R.C.J. Somerville, 2000: Implications of microphysics for cloud-radiation parameterizations: lessons from TOGA COARE. *J. Atmos. Sci.*, **57**, 161--183.

Macke, A., J. Mueller, and E. Raschke, 1996: Single scattering properties of atmospheric ice crystals. *J. Atmos. Sci.*, **53**, 2813-2825.

McFarquhar, G.M., and A.J. Heymsfield, 1997: Parameterization of tropical cirrus ice crystal spectra and implications for radiative transfer: results from CEPEX. *J. Atmos. Sci.*, **54**, 2187-2201.

McFarquhar, G.M., A.J. Heymsfield, A. Macke, J. Iaquinta, and S.M. Aulenbach, 1999: Use of observed ice crystal sizes and shapes to calculate mean scattering properties and multi-spectral radiances: CEPEX 4 April 1993 case study. *J. Geophys. Res.*, **104**, 31763-31779.

McFarquhar et al., 2002: A new parameterization of single-scattering solar radiative properties for tropical anvils using observed ice crystal size and shape distributions. *J. Atmos. Sci.*, In press.

Vogelman, A.M., and T.P. Ackerman, 1995: Relating cirrus cloud properties to observed fluxes: a critical assessment. *J. Atmos. Sci.*, **52**, 4285-4301.

Yang, P., K.-N. Liou, K. Wyser, and D. Mitchell, 2000: Parameterization of the scattering and absorption properties of individual ice crystals *J. Geophys. Res.*, **105**, 4699-4718.